A POLARIZATION APPROACH TO DETERMINING ROTATIONAL ANGLES OF A MORTAR

by

Muhammad Hassan Chishti

A thesis submitted to the Faculty of the University of Delaware in partial fulfillment of the requirements for the degree of Master of Science in Electrical and Computer Engineering

Summer 2010

A POLARIZATION APPROACH TO DETERMINING ROTATIONAL ANGLES OF A MORTAR

by

Muhammad Hassan Chishti

Approved: ____

Daniel S. Weile, Ph.D
Professor in charge of thesis on behalf of the Advisory Committee

Approved: ____

Kenneth E. Barner, Ph.D
Chair of the Department Electrical and Computer Engineering

Approved: ____

Michael J. Chajes, Ph.D
Dean of the College of Engineering

Approved: ____

Debra Hess Norris, M.S
Vice Provost for Graduate and Professional Education

This thesis is dedicated to,

My Sheikh Hazrat Maulana Mufti Muneer Ahmed Akhoon Damat Barakatuhum

My Father Muhammad Hussain Chishti

My Mother Shahida Chishti

ACKNOWLEDGMENTS

First and foremost, my all praise and thanks be to the Almighty Allah, *The Beneficent*, *Most Gracious, and Most Merciful*. Without His mercy and favor I would have been an unrecognizable speck of dust.

I am exceedingly thankful to my advisor Professor Daniel S. Weile. It is through his support, guidance, generous heart, and mentorship that steered me through this Masters Thesis. Definitely one of the smartest people I have ever had the fortune of knowing and working. I am really indebted to him for all that.

I would like to thank the Army Research Labs (ARL) in Aberdeen, MD for providing me the funding support to perform the research herein. Especially I would like to mention the name of Dr. Gary Katulka of ARL, whose support and guidance proved invaluable in this project.

I would also like to acknowledge Madhu Advani of Cornell University, who was part of our group during the summers of 07' and 08', for providing some very useful contribution towards this work. Never to forget my ever hardworking group mates, Xiaobo Wang and Yunqu Lin.

Most importantly, I would like to express my utmost and deepest gratitude towards my *Sehikh*, my parents, my sister Faiza, and my brother Farid. Without them on my side I would not have finished this endeavor successfully.

On a closing note, many thanks to my dear friends Syed Fahad Hussain and Dr. Masnoor-Ur-Rehman for their priceless support, and for listening to my whining!

TABLE OF CONTENTS

LIST OF FIGURES

ABSTRACT

The polarization of the electromagnetic wave transmitted by antenna beacons are used for estimating certain parameters associated with a projectile launched in free space. The development of a novel sensor based on the characteristics of a propagating polarized electromagnetic wave is presented in this thesis. In particular this thesis investigates how antenna laws can be effectively employed for the real-time and direct measurement of the geometrical orientation (attitude) of a mortar or missile launched in space with respect to a set of reference beacons.

This study begins by attempting to determine the location and orientation of a set of dipole antennas to be used as beacons and then builds on those results to move onto more complex antenna design and structures such as smart antennas. Results will show that the proposed scheme has potential as an attitude determination mechanism.

Chapter 1

INTRODUCTION

Electromagnetic theory has an incomparable importance in the understanding of scientific problems and has been an indispensable part of engineering analysis since Maxwell first proposed the complete theory in 1873 [1]. Wireless communications, remote sensing, circuit theory, and the modern marvels of optoelectronics all rely heavily on the fundamentals of electromagnetic theory and the tools and the applications that have sprouted from it.

Antenna fundamentals, which are an essential part of this thesis, emanate from and operate on the theory of electromagnetics. In particular, this thesis brings together several antenna design ideas to design an attitude sensor for a projectile. The projectile studied here is assumed to be a mortar, but this is not essential. The particular mortar model that was used approximates the size and shape of the mortar to give a better idea of the sort of interference to expect but different designs would not change the design procedure, which should be applicable to any projectile.

The primary idea proposed here is to place some antennas on the fired mortar and then utilize them to estimate the position and altitude parameters and also the rotational angles as the mortar rotates and spins in the air. All this is done with respect to a set of beacons, which are transmitting antennas, fixed at known locations on the ground. Since the field radiated by the beacons can be designed before hand, by measuring the fields they radiate the mortar can calculate some of its position/attitude variables.

This thesis, then, analyzes two parts of this problem. First, the basic theory is analyzed using ideal assumptions:

No mortar body to interfere with wave reception, perfect Hertzian dipoles whose voltage is directly proportional to a dot product with the field, and so on.

Second, practical problems that arise are discussed. In particular, we consider the design of practical antennas for the receivers on the mortar, and consider the interference of the mortar by using a commercial software package [2].

The remainder of this thesis will proceed as follows:

Chapter 1 gives the introduction of this thesis and what problem is being investigated.

Chapter 2 talks about the fundamentals of antenna and electromagnetic theory and how those laws are incorporated in this project.

Chapter 3 goes into the description and methodology of this polarization based sensor and some of the antenna parameters that are being computed.

Chapter 4 talks about the three dimensional rotation of the body and the geometric complications that are encountered while figuring out the rotational angles of the projectile.

Chapter 5 gives the description of the methodology of computing the three directional vectors associated with the projectile motion.

Chapter 6 described the mortar design and the simulations that were performed while placing antennas along different length of the mortar body.

Chapter 7 gives the details of a realistic antenna design, which in our case is a Broad-Band dual Polarized Aperture Coupled Patch Antenna.

Chapter 8 talks about how this problem could be approached using smart antennas.

Chapter 9 gives the summary and some of the future work being anticipated.

Chapter 2

FUNDEMENTALS OF ANTENNAS

2.1 Basic Electromagnetic Theory

To begin our discussion and introduce notation, we list Maxwell's Equations, the basic laws of electromagnetics.

Maxwell's equations describe the interaction between electromagnetic sources and fields, and may be written as [3]:

$$\nabla \times \mathbf{E} = -\frac{\partial \mathbf{B}}{\partial t} \tag{2.1}$$

$$\nabla \times \mathbf{H} = \mathbf{J}_i + \mathbf{J}_c + \frac{\partial \mathbf{D}}{\partial t} \tag{2.2}$$

$$\nabla \cdot \mathbf{B} = 0 \tag{2.3}$$

$$\nabla \cdot \mathbf{D} = q_{ev} \tag{2.4}$$

The definitions and units of the quantities are:

$\mathbf{E}$	=	Electric field intensity	(V/m)
$\mathbf{H}$	=	Magnetic field intensity	(A/m)
$\mathbf{D}$	=	Electric flux density	(C/m^2)
$\mathbf{B}$	=	Magnetic flux density	(Wb/ m^2)
$\mathbf{J}_i$	=	Impressed electric density	(A/ m)
$\mathbf{J}_c$	=	Conduction electric current density	(A/ m^2)
q_{ev}	=	Electric charge density	(C/ m^2)

In addition to the basic Maxwell equation, power considerations are often important in analyzing antennas. The Poynting vector as given by equation 2.5,

$$\mathbf{P} = \mathbf{E} \times \mathbf{H} \tag{2.5}$$

describes power flow in W/m^2 as is shown in textbooks on electromagnetic theory.

In the analysis of the radiation problems, the usual procedure involves specifying the sources and then computing the fields radiated by the sources. By introducing an auxiliary function, known as the vector potential, it is possible to simplify the analytical process of finding **E** and **H**. The vector potential **A** for an electric current source **J** is described by the following relationship:

$$\mathbf{A}(x, y, z) = \frac{\mu}{4\pi} \iiint_V \mathbf{J}(x', y', z') \frac{e^{-jkR}}{R} dv' \tag{2.6}$$

In this equation μ represents the permeability, and *R* represents the distance from any point in the source to the observation point. The primed coordinates represent the source; the unprimed coordinates represent the observation point.

The electric and magnetic fields are related to the vector potentials by using the following equations:

$$\mathbf{E} = -j\omega\mathbf{A} - \frac{1}{j\omega\mu\varepsilon} \nabla\nabla \cdot \mathbf{A} \tag{2.7}$$

$$\mathbf{H} = \frac{1}{\mu} \nabla \times \mathbf{A} \tag{2.8}$$

In the far field, which is generally the region of interest for antennas, these equations simplify further:

$$
\begin{aligned}
\mathbf{E}_r &= 0 & \mathbf{H}_r &= 0 \\
\mathbf{E}_\theta &= -j\omega\mathbf{A}_\theta & \mathbf{H}_\theta &= -\frac{\mathbf{E}_\phi}{\eta} \\
\mathbf{E}_\phi &= -j\omega\mathbf{A}_\phi & \mathbf{H}_\theta &= +\frac{\mathbf{E}_\theta}{\eta}
\end{aligned}
\tag{2.9}
$$

All of these equations are used later in this thesis to model antenna behavior. We now discuss different antennas that are available for incorporation into our system.

2.2 Types of Antennas

Antennas act as transitional devices that assist the transport of electromagnetic energy. Whether the antenna acts as a transmitter or receiver, the antenna acts as an intermediary device that converts between guided and free space modes of propagation. Different types of antennas provide different radiation patterns and radiating characteristics for use in different application; some of these devices include: wire antennas, loop antennas, array antennas, aperture antennas, microstrip antennas, smart antennas, and horn antennas.

Wire antennas are most well known to the layman, as they are readily visible on my platforms such as ships, aircraft, automobiles, and buildings [4]. Wire antennas, linear or curved, are some of the oldest, cheapest, and most versatile antennas in use today. Because of their simplicity, they make a good starting point for our particular investigations.

The simplest form of the wire antennas is the Hertzian dipole. Although it is not a very practical antenna, it can be used as a theoretical building block for more intricate geometries and structures. The determination of the polarization rotational angles for this project begins with the simulations of the dipoles as the mounted structures on the projectile and codes are written in accordance with that before going into more realistic and complicated antenna designs.

Another important type of antenna in applications is the array. Array antennas are necessary in the achievement of high directivity. Arrays are also useful since individual control of elements allows for steering and direction finding applications. Arrays will be discussed later in this work because of these properties.

Finally we examine patch antennas in later chapters. The microstrip patch antenna comes in a variety of designs, which allow designers to use different feeding methods, a planar or conformal configurations, and integration into various applications. Some of these applications include: high-performance aircraft, spacecraft, satellites, missiles, card, and even cell phones. The basic structure of a microstrip antenna consists of a metallic patch on top of a grounded substrate. In this project the microstrip antennas are used as a more prudent alternative to wire antennas because of their simplified geometry for placing them on a projectile.

Chapter 3

POLAR SENSOR NAVIGATION SYSTEM DESCRIPTION

3.1 General Description

As mentioned in the introduction, the purpose of this work is the creation of a system that is able to deduce information about a projectile by measuring the polarization of an incident electromagnetic wave. The most important parameters to measure are the three rotational angles associated with this projectile. In this chapter we described both the desired unknowns and the general layout of the system we will use to measure them.

The primary fixed component of the system is a beacon antenna that is fixed at the origin. Three orthogonal receiving antennas are attached to the launched projectile, which detect the polarization of the transmitted electromagnetic wave by the beacon and collect the data. The information so obtained is to be used to compute the three rotational angles. These angles are generally known as the yaw ψ, pitch θ, and roll angle Φ, and are illustrated in Figure 1. The basic idea behind the computation scheme is that because the antenna receives a voltage proportional to the projection of the electric field vector onto it, from the projection of a known electric field on three orthogonal antennas, the attitude of the projectile can be computed.

3.2 Overview of Computer Implementation

To simulate this then requires a suite of techniques to compute the energy or voltage received by an antenna due to a wave created by another antenna. To make the simulations complete, the code should have the capability of simulating antennas arbitrarily far apart, with arbitrary relative attitude. In general this could be a very complicated problem, but we assume that the antennas are in each other's far fields (a near certainty in practice) and that their far field is known, and unaffected by the environment.

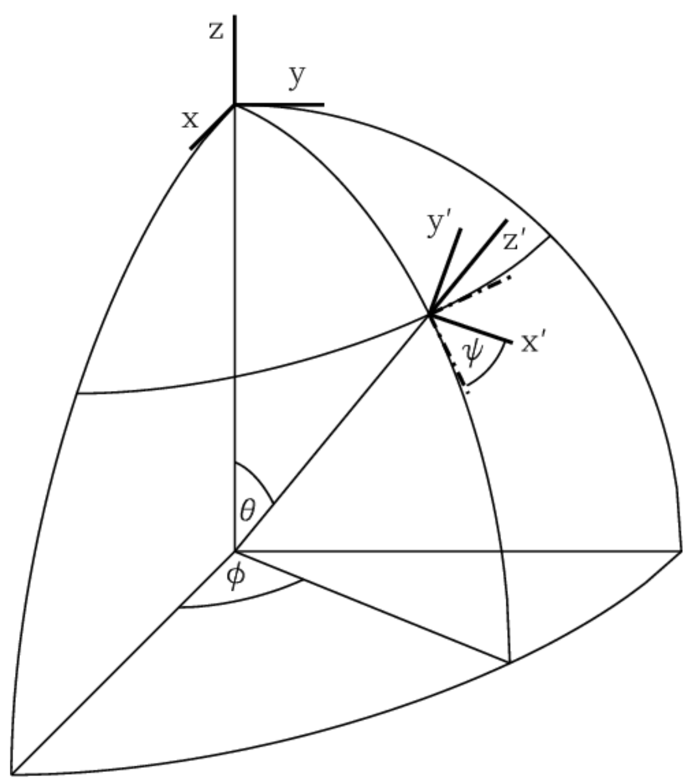

Figure 1. The Three Rotational Angles: Yaw angle ψ, Pitch angle θ, and Roll angle Φ.

Thus, it is assumed that the user provides far field values for the pattern in the following format:

$$\mathbf{E}(\theta,\phi) = \frac{e^{-jkr}}{4\pi r}\left[\hat{\theta}E_{\theta}(\theta,\phi) + \hat{\phi}E_{\phi}(\theta,\phi)\right] \tag{3.1}$$

This is the equation for the electric field pattern and the θ and ϕ are the spherical coordinates and it is a function of E_{θ} and E_{ϕ} which are the field components in the respective directions. It does not matter how these values are computed, just that the user provides codes that can compute E_{θ} and E_{ϕ} for any value of θ and ϕ.

From this information, all of the properties necessary for the simulation can be computed. The abilities of the simulation codes are detailed in the remainder of this chapter.

3.3 Friis Transmission Equation

There are two primary ways of computing the interaction between two antennas, and the primary difference between them is the physical variable with which they work. The first method is based on the Friis Transmission formula, and directly computes the power received by one antenna in terms on the power transmitted by another. The second method is based on the concept of vector effective length, and it works by computing the voltage generated at the terminals of the receiver due to a known voltage in the transmitter. We discuss the Friis formula here, and the vector effective length in the next section.

The Friis formula is perhaps the single most well known equation of antenna theory, and it can be found in any textbook on the subject. The Friis transmission equation can be written as follows:

$$\frac{P_r}{P_t} = e_{cdt} e_{cdr} (1 - |\Gamma_t|^2)(1 - |\Gamma_r|^2) \left(\frac{\lambda}{4\pi R} \right)^2 D_t(\theta_r, \phi_t) D_r(\theta_t, \phi_r) |\hat{\rho}_t \cdot \hat{\rho}_r|^2 \tag{3.2}$$

Where, P_r is the power received, P_t is the power transmitted, Γ_t and Γ_r are the reflection coefficients for the transmitting and receiving antenna, the term $\left(\frac{\lambda}{4\pi R} \right)$ is called the free-space loss factor, λ is the free space wave length, R is the distance between the two antennas, D_t and D_r are the directivity of the two antenna, which is defined as the radiation intensity in a given direction from the antenna to the radiation intensity averaged over all directions. The codes were written to compute these directivities. The terms e_{cdr} and e_{cdt} are the antenna efficiency constants.

For our purposes, the most important quantity in the Friis formula is the polarization loss factor, which accounts for the loss due to misalignment of the receiver with the polarization of the wave launched by the transmitter. Mathematically,

$$\text{PLF} = |\hat{\rho}_t \cdot \hat{\rho}_r|^2 \qquad (3.3),$$

where, $\hat{\rho}_r$ and $\hat{\rho}_t$ are the polarization unit vectors for the transmitted and received wave. (Note that these vectors can be complex if the incident wave is circularly or elliptically polarized). Because the PLF is maximized when the polarizations are aligned and minimized when they are orthogonal, the Friis formula (and our Friis formula code) can be used to compute the protection of the wave generated by the beacon onto an antenna on the projectile.

3.4 Vector Effective Length

The only difficulty with the Friis formula approach is that it lacks phase information because it only involves power. Because the vectors involved in the PLF calculation are complex, this leaves some ambiguity in the projection computation. For instance, if a linearly polarized receiving antenna receives half of the power available at its location in space, we cannot discern from this if the impinging wave is circularly polarized or if the receiver is merely misaligned. In general, more information is available in the terminal voltage, so we now turn to the definition and computation of the vector effective length $\mathbf{I}^{eff}$.

An antenna has effective length $\mathbf{I}^{eff}$ if it produces an open circuit voltage

$$V_{oc} = \mathbf{E}^{inc} \cdot \mathbf{I}^{eff} \tag{3.4}$$

V_{oc} $\mathbf{I}^{eff}$ when excited by an incident field $\mathbf{E}^{inc}$

$$\mathbf{E}^{inc} = -j\eta \frac{kI_{in}}{4\pi R} l_e e^{-jkr} \tag{3.5}$$

Given this information, we are ready to begin creating simulations.

Chapter 4

GEOMETRIC COMPLICATIONS

4.1 Introduction

The rotational angles associated with a mortar launched in free space constitute quite a bit of geometric complications. Describing rotation in three dimensions is complicated especially when we are dealing with two different sets of coordinate systems. In our case we have a coordinate system attached to the radiating antenna that is fixed at the origin. The other coordinate system is the one, which is associated with the antennas that are mounted on the constantly rotating projectile. Coordinate system attached with the antenna fixed at the origin is termed as the global coordinate system and the one related to the antennas on the projectile is referenced as the local coordinate system. Both of these systems have different origins and what makes them even more complicated is that they are being rotated with respect to each other.

A need arises to write codes that would successfully be able to compute the three-dimensional angular orientation of the projectile with respect to the global coordinate system and also at the same time be able to convert between certain angular notations. Also the codes were written that were able to convert between spherical coordinates, rectangular coordinates, and polar coordinates.

4.2 Euler Angle Rotations

Euler angles are used to describe the orientation of a rigid body in three-dimensional space when it is subjected to a sequence of rotations [5]. There are two different frames of reference or coordinate system that we ascribe in defining the Euler rotations. There is a fixed global frame that is rigidly attached to an object, which in our case is the antenna fixed at the origin and then a local frame is defined that is rigidly attached to an object. The local and global frames initially coincide and then subsequent rotations are performed with respect to the local frame, so that when an object is rotated the frame rotates with it. The rotations angles in this case are known as Euler angles. The goal is basically to describe the orientation of a final rotated system relative to some initial coordinate system.

The fixed frame can be denoted as x, y, z while x', y', z' indicate the position after the first rotation as indicated by the argument over the coordinates. The three rotational angles are termed as yaw, pitch, and roll and are denoted by ψ, θ, Φ, respectively. There could be different conventions in Euler angles calculations depending on about which axis is rotated first and in what order. The convention used in our codes is the *z* convention which means that the body is first rotated about *z* axis, then *y* axis and finally about *x* axis.

The relationship between the rotation matrix $[\mathbf{R}]$ and the rotational angles is given as follows:

$$\mathbf{R} = \begin{pmatrix} \cos\theta\cos\phi & -\cos\theta\sin\phi & \sin\theta \\ \cos\psi\sin\phi + \sin\psi\sin\theta\cos\phi & \cos\psi\cos\phi - \sin\psi\sin\theta\cos\phi & -\sin\psi\cos\theta \\ \sin\psi\sin\phi - \cos\psi\sin\theta\cos\phi & \sin\psi\cos\phi + \cos\psi\sin\theta\cos\phi & \cos\psi\cos\theta \end{pmatrix} \quad (4.1)$$

$$\mathbf{R} = \begin{pmatrix} r_{11} & r_{12} & r_{13} \\ r_{21} & r_{22} & r_{23} \\ r_{31} & r_{32} & r_{33} \end{pmatrix} \tag{4.2}$$

From equation 4.1 and 4.2, Euler angles can be computed and are given by the following set of equation:

$$\text{Yaw angle } \psi = \tan^{-1}\left(-\frac{r_{23}}{r_{33}}\right) \tag{4.3}$$

$$\text{Pitch angle } \theta = \tan^{-1}\left(\frac{r_{13}}{-r_{23}\sin\psi + r_{33}\cos\psi}\right) \tag{4.4}$$

$$\text{Roll angle } \Phi = \tan^{-1}\left(\frac{r_{21}\cos\phi + r_{31}\sin\phi}{r_{23}\cos\psi + r_{32}\sin\psi}\right) \tag{4.5}$$

4.3 Quaternion Rotation

Quaternions, invented by W.R.Hamilton in 1843, prove to be useful for computing the product of sequential rotations about arbitrary axis and subsequently extracting the equivalent rotation angle and axis [6]. Rotations described by this method are simpler to compose and implement as compared to the Euler angles.

Rotation about an arbitrary axis in space is the most general form of a rotation transformation. A unit vector $\hat{\mathbf{a}}$ is defined as the axis about which the rotation to take place, and the angle of rotation by α. The rotational angle can be defined by the following equations:

$$R = \begin{pmatrix} \cos\alpha + \hat{a}_x^2(1-\cos\alpha) & -\hat{a}_z\sin\alpha + \hat{a}_x\hat{a}_y(1-\cos\alpha) & \hat{a}\sin\alpha + \hat{a}_x\hat{a}_z(1-\cos\alpha) \\ \hat{a}_z\sin\alpha + \hat{a}_x\hat{a}_z(1-\cos\alpha) & \cos\alpha + \hat{a}_y^2(1-\cos\alpha) & -\hat{a}_x\sin\alpha + \hat{a}_y\hat{a}_z(1-\cos\alpha) \\ -\hat{a}_y\sin\alpha + \hat{a}_x\hat{a}_z(1-\cos\alpha) & \hat{a}_x\sin\alpha + \hat{a}_y\hat{a}_z(1-\cos\alpha) & \cos\alpha + \hat{a}_z^2(1-\cos\alpha) \end{pmatrix}$$

(4.6)

Where,

$$\hat{\mathbf{a}} = \hat{a}_x^2 + \hat{a}_y^2 + \hat{a}_z^2 = 1 \qquad (4.7)$$

This rotation can now be described by the quaternion transformation as follows:

$$R = \cos(\alpha / 2) + \sin(\alpha / 2)\hat{\mathbf{a}} \qquad (4.8)$$

The rotation transformation can be obtained from either of these methods and the codes were written for both forms separately. Also another important piece of code was written to transform between the Euler angle methodology and the one based about arbitrary axis and quaternion rotations.

Chapter 5

POLARIZATION BASED ATTITUDE SENSOR METHODOLOGY

5.1 Introduction

This chapter includes the discussion that how the information obtained from the polarization of the transmitting and receiving antennas, antenna parameters, and the three-dimensional geometric computations and complications, that were discussed earlier can now be effectively employed in determining the three rotational angles of the mortar.

A radiating antenna is fixed at the origin with coordinate system x, y, z. In our case this antenna is a Hertzian dipole located at the origin that does the job of a beacon, which the mortar used the signal of to calculate its position. This beacon radiates an elliptically polarized wave along the x-axis, as described by the following equations:

$$\mathbf{E}(\mathbf{r}, w) = (\hat{\mathbf{x}} - 2j\hat{\mathbf{y}})e^{-jkz} \tag{5.1}$$

$$\mathbf{E}(\mathbf{r}, t) = \hat{\mathbf{x}}\cos(wt - kz) + 2\hat{\mathbf{y}}\sin(wt - kz) \tag{5.2}$$

Three linearly polarized wire antennas are mounted on the projectile with a coordinate system x', y', z' to receive the electromagnetic field as radiated by the beacon. The projectile is launched within the main beam of the radiating antenna. The plane of the ellipse with the sense of rotation provides us with one axis. The major and minor axes of the ellipse can help us determining the other axes within single sign ambiguity.

5.2 Direction Vectors

The position and the orientation of the projectile can now be determined by figuring out the three direction unit vectors $\hat{x}, \hat{y}, \hat{z}$ in terms of the coordinate system of the mortar. This was done by first creating a vector **P** by stacking the results of our measurements of the received field.

$$\mathbf{P} = a\hat{\mathbf{x}}' + b\hat{\mathbf{y}}' + c\hat{\mathbf{z}}' \tag{5.3}$$

Now since we know that the plane of the ellipse is normal to the x-axis and the real and the imaginary part of **P** are in the plane, the direction vector $\hat{\mathbf{x}}$ would now the cross product of real and imaginary parts of **P**.

$$\begin{aligned}
&\mathbf{r} = \mathrm{Re}\{\mathbf{P}\}, \mathbf{s} = \mathrm{Im}\{\mathbf{P}\} \\
&\mathbf{x} = \mathbf{s}(\hat{\mathbf{x}}', \hat{\mathbf{y}}', \hat{\mathbf{z}}') \times \mathbf{r}(\hat{\mathbf{x}}', \hat{\mathbf{y}}', \hat{\mathbf{z}}') \\
&\hat{\mathbf{x}} = \frac{\mathbf{x}}{|\mathbf{x}|}
\end{aligned} \tag{5.4}$$

The direction vector $\hat{\mathbf{z}}$ can now be obtained by following set of equations:

$$\begin{aligned}
&\tau_o = \frac{1}{2}\tan^{-1}\left[\frac{2\mathbf{r}\cdot\mathbf{s}}{\mathbf{s}^2 - \mathbf{r}^2}\right] \\
&\tau_1 = \tau_o + \frac{\pi}{2} \\
&\mathbf{P} = \mathbf{r} + j\mathbf{s} \\
&\mathbf{P}_o = \mathbf{P}(\tau_o) \\
&\mathbf{P}_1 = \mathbf{P}(\tau_1) \\
&\mathbf{P}_{\max} = \arg\max|\mathbf{P}| \\
&\hat{\mathbf{z}} = \pm\frac{\mathbf{P}_{\max}}{|\mathbf{P}_{\max}|}
\end{aligned} \tag{5.5}$$

The final direction vector is the easiest of all and it is simply the cross product of the two direction vectors, calculated earlier. It is given as follows:

$$\hat{\mathbf{y}} = \hat{\mathbf{z}} \times \hat{\mathbf{x}} \tag{5.6}$$

5.3 Roll Angle

It is assumed that the projectile in our case remains within the main beam of the beacon or the radiating antenna. So the roll angle Φ is the most important rotational angle to be determined. Roll angle Φ is the dot product of the direction of a receiver and the polarization of the signal, which is the fraction of the signal picked up by a receiving antenna.

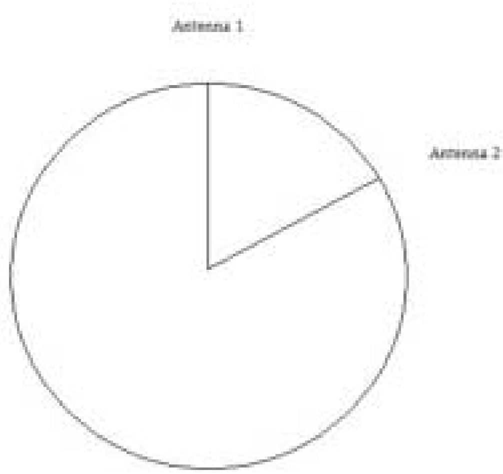

Figure 2. Determination of the Roll Angle Φ by the Dot-Product of the Receiver and the Polarization of the Transmitted Antenna.

By looking at the voltage ratio between the two receiving antennas, we can determine with 180-degree uniqueness, the angle of the missile with respect to the beacon’s direction of polarization. In order to determine this voltage ratio, we need both the magnitudes and the relative phase of the two oscillating voltages received by the antennas. The magnitude could be determined by applying Random Moment Sampling (RMS) and the phase difference could be determined relatively inexpensively by using slow data reading.

Using the basic antenna law and parameters that were discussed earlier, we can determine the voltage received by one antenna when another antenna radiates if we know the field patterns of both antennas. Thu this would enable us to determine the voltage that would be received by two of the antenna the missile, at 60-degree spacing from each other.

Using simple trigonometry and the assumption that, approximately, the only real difference the antennas was their polarization (i.e. Electric field reaching antenna and antenna properties are the same) the angle of the missile was back calculated with respect to the beacon’s polarization angle.

$$\Phi = -\left((\tan^{-1}\left(\frac{2V_2 - V_1}{\sqrt{3V_1}} \right) + 90) \pm 90 \right) \tag{5.7}$$

Chapter 6

MORTAR DESIGN AND SIMULATIONS

6.1 Mortar Design 1

The mortar design that was used in this project approximates the size and shape of the mortar to give us a better idea of the sort of interference to expect. The exact dimensions of the mortar were a classified data only known the military. However simply for experimental purposes a mortar of length 1.5 feet and a diameter of 60 mm was designed for simulations. An electromagnetic simulator FEKO was used to for the mortar design and simulations and also for the antenna design. The following figure shows of the mortar that was designed in Cad FEKO for simulation purposes.

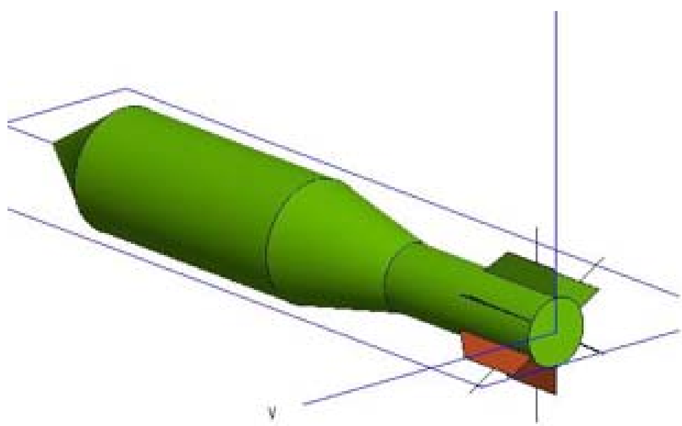

Figure 3. Design 1: Mortar Missile in CadFEKO. Antennas are placed on the fins for this design.

In this first design the antenna are placed on the fins of the missile. Either three or six antennas are necessary in this case to preserve symmetry. As far as the frequency is concerned most of the simulations were run around a frequency of 3 GHz. However just for the experimental purposes the design was also simulated at a frequency of as low as 500 MHz.

The programming language of MATLAB was used to simulate the actual mortar motion. The far-field data for the missile was then used in FEKO (the electromagnetic simulator), and a bi-linear interpolation code written to determine the missile's entire far-field solution. The far-field from this first design and from the beacon is depicted in the Figure 4 and 5.

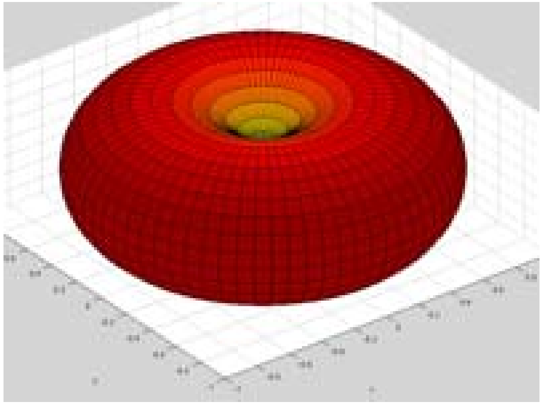

Figure 4. Electric Field Radiated by the Hertzian dipole, which acts as the Beacon.

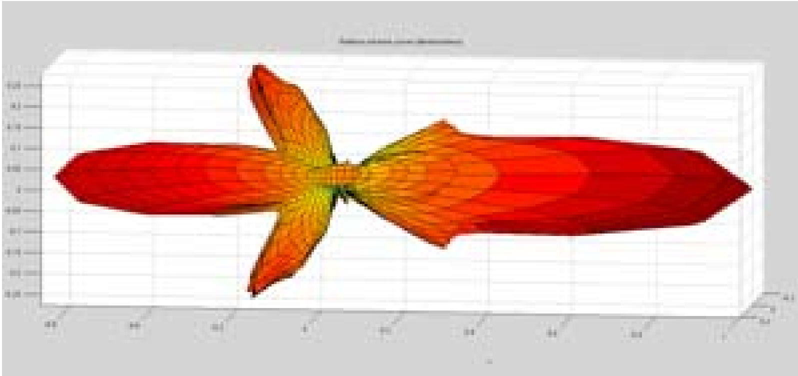

Figure 5. Design 1: Electric Field Radiated by the Missile as Determined From FEKO Simulation.

6.2 Mortar Design 2

In this design the antennas are placed further up the neck of the missile and the same simulations were run using the Cad FEKO simulator. The following figures show the missile design and also the far field produced by it.

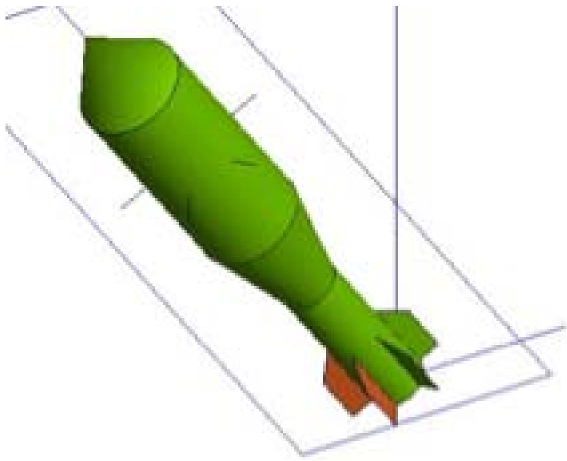

Figure 6. Design 2: Mortar Missile in CadFEKO. Antennas are placed farther up the neck.

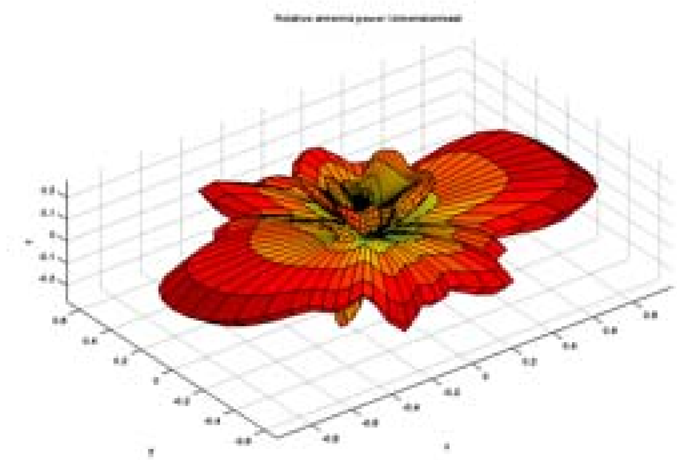

Figure 7. Far field Produced by Mortar Missile Design 2.

6.3 Simulation Results

A simulation program is then written in which the missile is placed somewhere on the coordinate system and its roll angle is varied, as if it were rotating in real time with a constant angular velocity. The roll angle is then back-calculated using the voltages read by the antenna attached to the missile. This simulation is very useful in the sense that it enables us to plot the actual angle as well as the predicted angle with time in order to see how close the prediction would going to be. This simulation is also applied to the data about where the missile was in the past to predict all 360-degrees of its rotation.

6.3.1 Mortar in Direct Line from the Dipole Transmitter

The graph in Figure 8 shows us this plot of the predicted and actual roll angle with respect to time. This model shows the best-case theoretical situation in which there is no noise and the mortar is in a direct line from the dipole transmitter. The two situations are off by less than one degree everywhere.

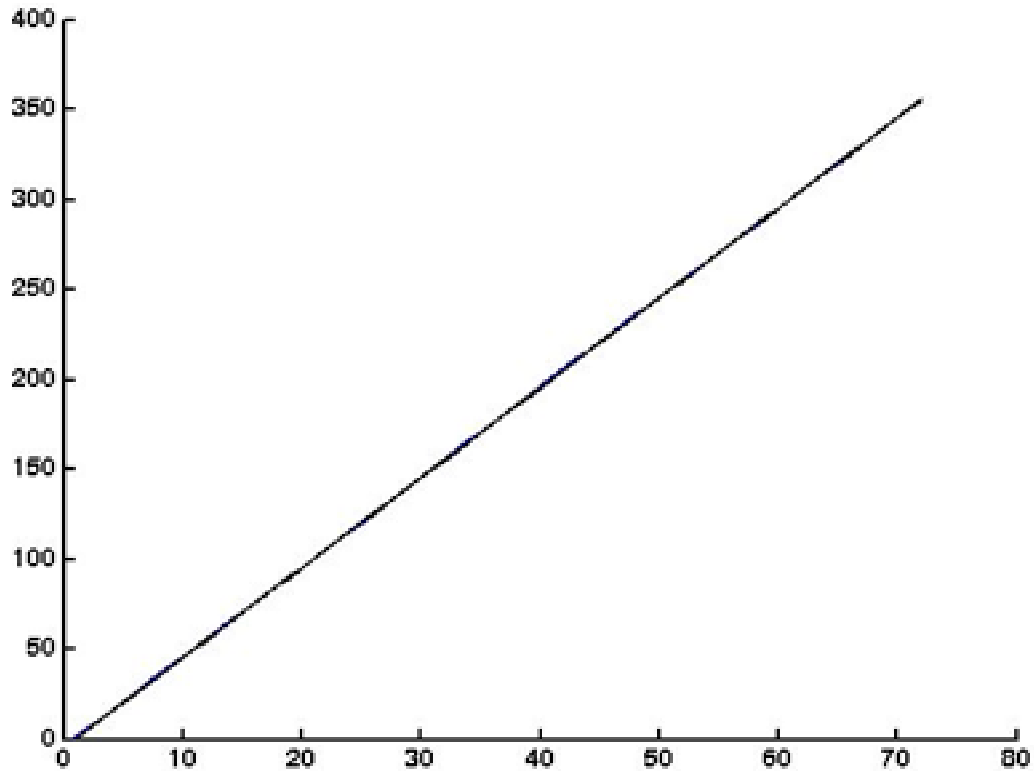

Figure 8. The Calculated and the Actual Roll Angle of the Missile, Given a Constant Angular Velocity, plotted together.

6.3.2 Mortar 10 Degree off Direct Line

The following figure shows the simulation results with mortar being 10-degree off from the line of the dipole transmitter or beacon.

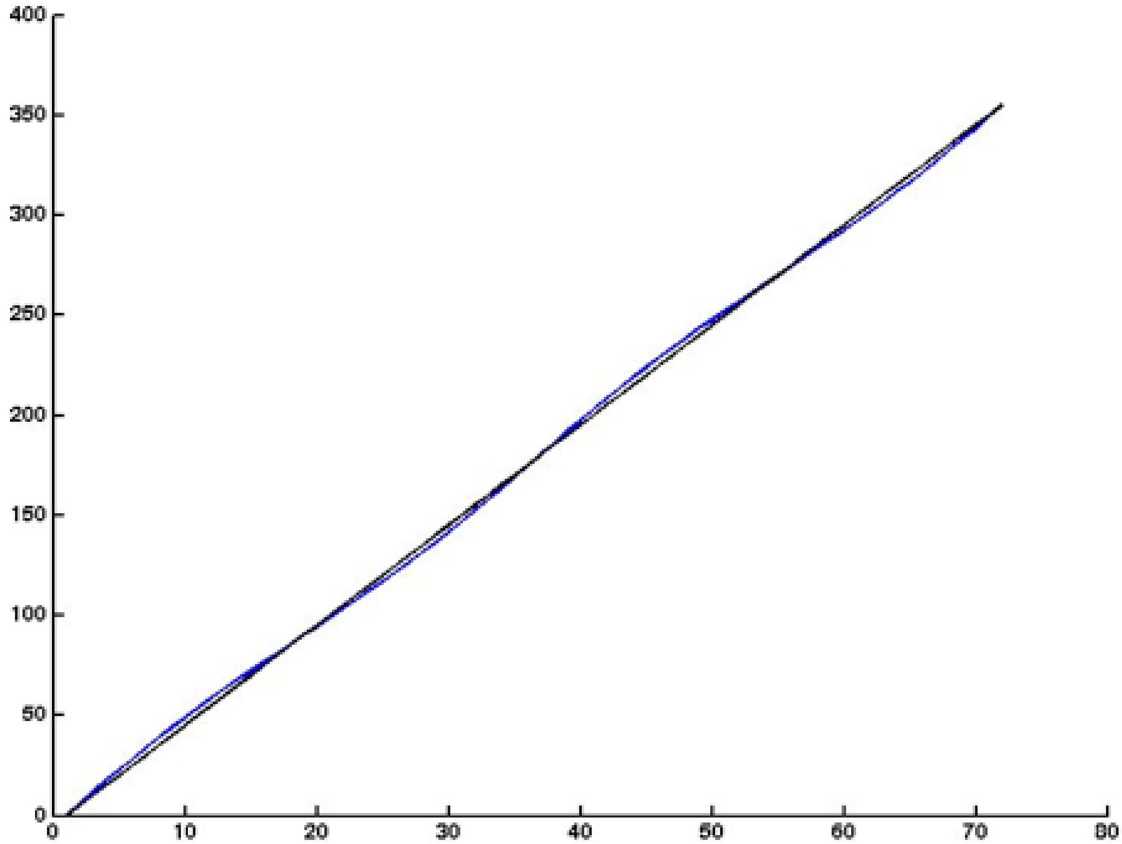

Figure 9. Actual versus calculated Roll Angle for Missile with a 10-degree rotation around the y-axis.

6.3.3 Mortar 20 Degree off Direct Line.

Figure 10 also shows the simulation results of the actual roll angle versus the predicted roll angle, however this time the mortar being 20-degrees off the main beam or direct line from the beacon.

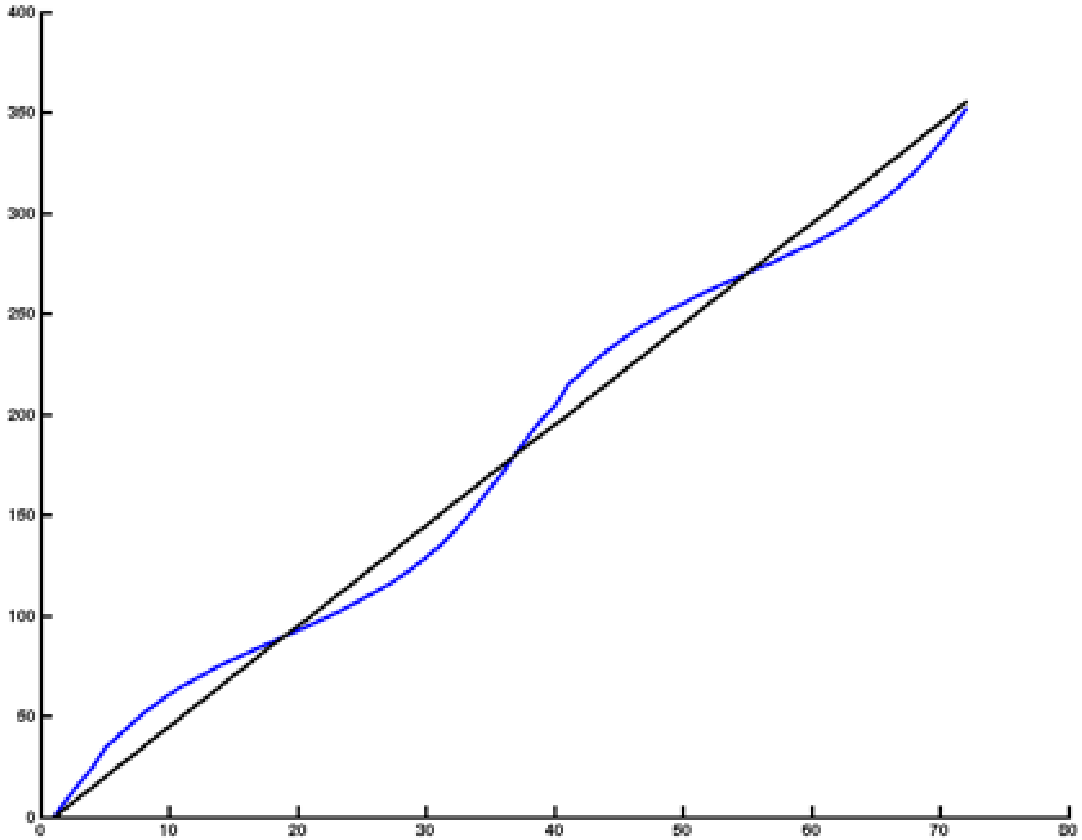

Figure 10. Actual versus calculated Roll Angle for missile with a 20-degree rotation around the y-axis.

6.4 Comparison of Mortar Design 1 & 2

The graph in Figure 11 shows a comparison of the two models of mortars with antennas placed on the fins, and the other model where antenna are placed farther up the neck. The black line in both the graphs shows the theoretical values, and the blue line depicts the simulated results for both the models.

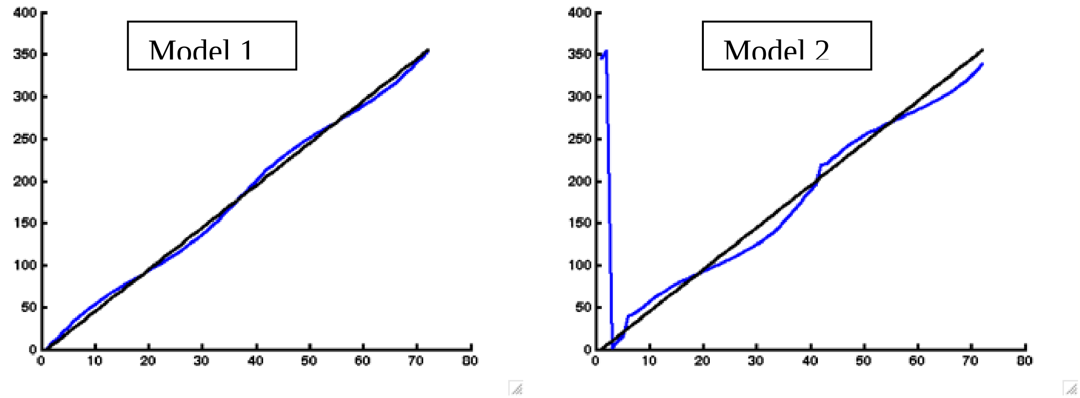

Figure 11. Comparison of Mortar Design 1 and 2.

From the simulation results and the calculation it is observed that the model of the mortar with antenna placed at the fins is better than the one where antennas are placed farther up the neck, implying that the shape of the mortar has less effect on the signal when antenna are mounted on the fins.

The second mode is more sensitive to the angle of the mortar, with the far-field of the missile is turned 15-degrees about the y-axis, we see more discrepancy when the antennas are farther along the neck of the mortar. This solution does predict that the mortar rotation angle to good accuracy in special cases but in other cases, more work would have to be done to improve accuracy.

6.5 Design Issues

There are a few practical design limitations that need to be taken into consideration in this entire design of the polarization based attitude sensor.

The wire antennas that are being placed on the mortar do not constitute a very practical approach for a missile that is being shot out of a gun. In a field where such mortars are being used it is simply not a good idea to have wires sticking out of its sides. Some special design would be necessary for this to work and that would be discussed later in the chapter that talks about some practical antenna design.

Real-world noise and disturbance would also have an effect on the system and that could prove to be very disruptive. These aspects have not been taken into consideration for our design. This design of our polarization sensor does not provide us any information about the velocity, position, and phase of the projectile.

6.6 Off-beam Problem

While designing this navigation system, it has been assumed that the projectile has to remain within the main beam of the radiating antenna in order to receive any signal. All the simulations that have been carried out and the codes that have been written are based on this assumption. Anything off the main beam and all bets are off.

This assumption could best be understood by looking at Figure 12.

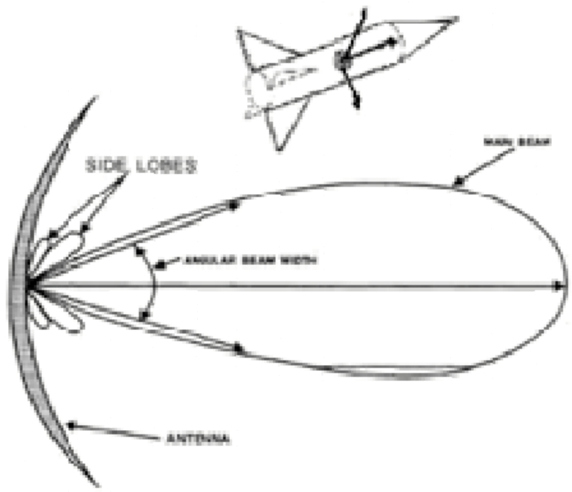

Figure 12. Main Beam of the Radiating Antenna and the Side Lobes. Projectile has to remain within the main beam.

The polarization purity is lost as we move out of the direct line of the missile, and for this reason this idea may prove to be impractical in a real world situation, where the angle of the missile is constantly changing and the missile will simply not be in-line with the beacon at all times.

6.7 Advantages

The system is very robust and also inexpensive. For such measurements, the GPS signals are also available, but are not accurate enough for many applications; the signal may not be available at all times, cannot be used effectively and accurately measure angular orientation and is also subject to jamming. One of the main advantages of this kind of polarization sensor is that the measurements of position and orientation relative to the reference antenna or the beacon is direct, and therefore prone to less error when used for control purposes.

Other advantages of such orientation sensor is that by using reference sources with high enough RF frequencies, the antenna design could be made very small and may even be embedded in the structure of the object. In addition, the reference antenna may be positioned very far, even several miles, away from the projectile. This kind of sensor also consumes very low power.

Only one kind of sensor is being employed in the entire design. Also no other information about the antenna is required other the polarization on the main beam. This makes it less sensitive to noise from reflections and absorption.

Chapter 7

REALISTIC ANTENNA DESIGN

7.1 Introduction

The simulations that have been carried and the codes that have been written for the design of our polarization sensor navigation system have assumed wire antennas being placed on the mortar. However wire antenna may not be practical structures to put on a missile that is being shot out of a gun. A more realistic antenna design is required that could relatively be easy to embed with the body of the projectile and also has a more directive electric field radiation pattern. Microstrip patch antenna could prove to be a very prudent solution to this problem as they cover less surface area and they offer relatively easy and practical integration with the mortar.

7.2 Microstrip Patch Antennas

Before going into the description of the actual type of the microstrip patch antenna that was used in our project, a short description of what patch antennas are is presented here in this section.

The microstrip patch antenna is nothing more than a radiating patch on one side of a dielectric substrate and a ground place on the opposite side as shown in Figure 13 [3].

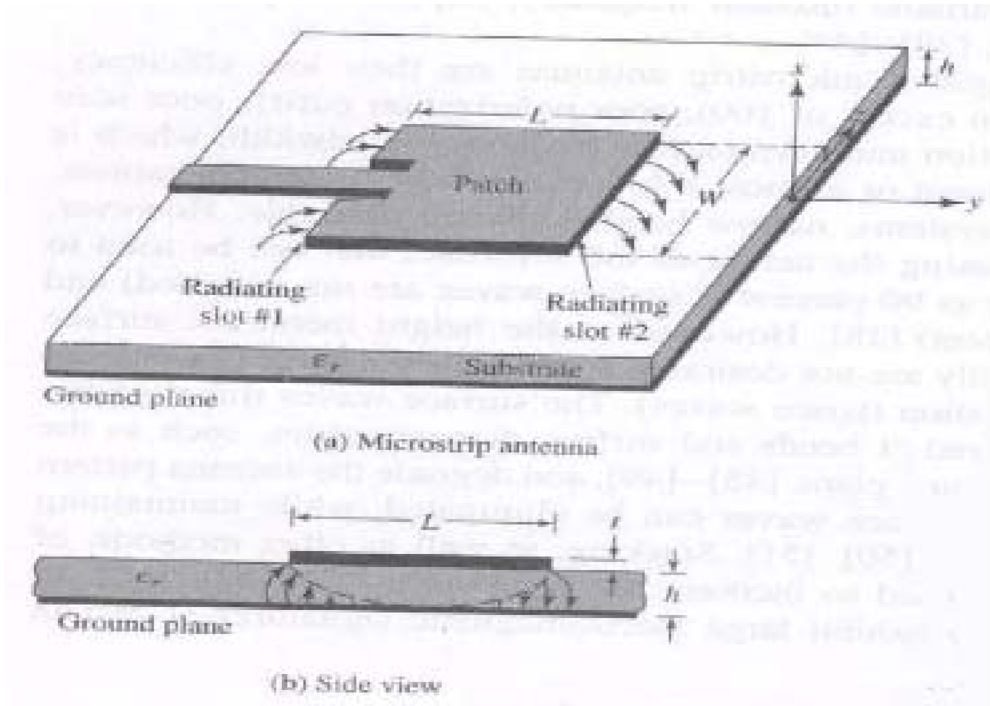

Figure 13. Basic Microstrip Patch Antenna Configuration [3].

Usually the patch conforms to some geometric shape such as a square, rectangle, circle, triangle, ellipse, or some other common shape. This simplifies analysis and allows for a better prediction of antenna performance. A rectangular patch of length L usually retains dimensions of $0.3333\lambda_o < L < 0.5\lambda_o$, where λ_o is the free space wavelength. The patch thickness is much smaller than the free space wavelength such that $t << \lambda_o$ (where t is the patch thickness). The dielectric substrate thickness h is usually falls in the range $0.003\lambda_o < h < 0.05\lambda_o$. Typical dielectric constants of the substrate (ε_r) lie in the range $2.2 \leq \varepsilon_r \leq 12$ [7]. Fringing fields between the patch edge and ground plane provide the fundamental radiating mechanism for microstrip patch antennas. A thick dielectric substrate having a low dielectric constant creates an antenna with better efficiency, larger bandwidth, and better radiation; however, this configuration leads to larger antenna dimensions. To design a compact microstrip patch antenna, a substrate with a higher dielectric constant should be employed, but using a higher dielectric constant results in a less efficient antenna and narrower bandwidth. Thus, a compromise must be reached between antenna dimensions and antenna performance. A typical frequency response of a microstrip patch antenna is shown in Figure 14. The radiation pattern characteristics are shown in Figure 15. Figure 15 shows the moderately directive properties of a single patch antenna.

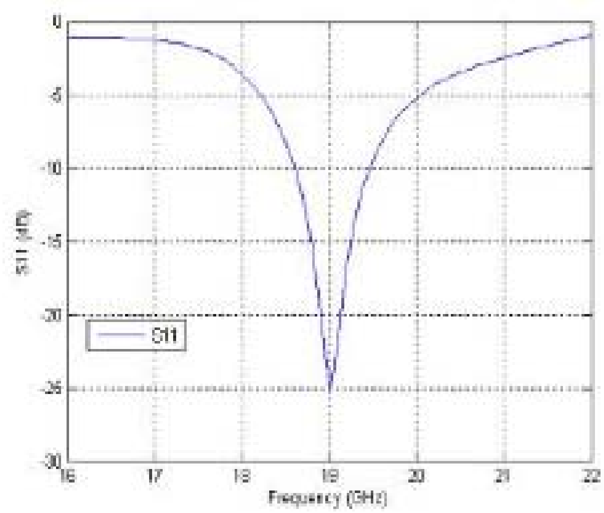

Figure 14. Typical Microstrip Patch Antenna Return Loss.

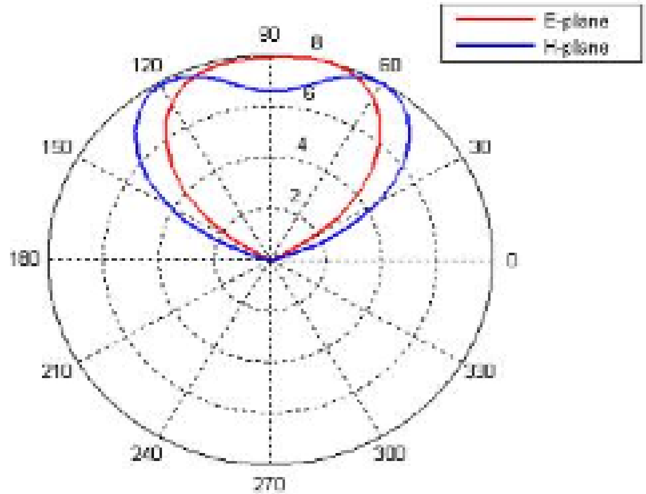

Figure 15. Predicted E- and H-plane Patterns of a Rectangular Microstrip Patch.

7.3 Advantages and Disadvantages

Microstrip patch antennas provide many enviable advantages for wireless applications. They have found their niche in many communications applications because of their low profile structure. Microstrip patch antenna can be found in high-performance aircraft, spacecraft, satellites, missiles, cars, and cell phones. Some of the advantages include: 1) light weight and low volume, 2) low profile planar configuration which be easily made conformal to the host surface, 3) low fabrication cost, 4) supports linear and circular polarizations, 5) the adeptness to be easily integrated with microwave circuits, 6) the efficacy of dual and triple frequency operations, and 7) mechanically robust when mounted on rigid surfaces. Some of their major disadvantage include: 1) narrow bandwidth 2) low efficiency, 3) low gain, 4) low power handling capacity, and 5) surface wave excitation.

Microstrip patch antennas possess a very high antenna quality factor (Q), which represents the losses associated with the antenna. A large Q means the antenna will have narrow bandwidth and low radiation efficiency. Typically, radiation, ohmic, dielectric, and surface wave losses exist within the antenna. Increasing the thickness of the dielectric substrate will lower the Q, but as the thickness increases, an increasing fraction of the total power delivered by the source goes into a surface wave. Surface waves represent unwanted power loss since they cause the degradation of antenna characteristics by scattering fields at the dielectric bends.

7.4 A Broad-Band Dual Polarized Aperture Coupled Microstrip Patch Antenna

7.4.1 Introduction

The realistic antenna design that was realized as part of this project was that of a broad-bandwidth dual polarized aperture coupled microstrip patch antenna. This was due to its broad-bandwidth, high-isolation, low cross-polarization levels and low back-ward radiation levels [8]. Also this design provided us with a more realistic mounting situation on the mortar. For broad-bandwidth and easy integration with the remaining circuitry, it uses the aperture-coupled stacked patches. The corner feeding of square microstrip patches is applied and the coupling aperture is the H-shaped aperture.

A classical way to obtain a dual-polarized aperture-coupled microstrip antenna consists in cutting two offset orthogonal apertures in the feed-line ground plane. Each aperture excites the patch in a single direction. Investigations of patch excited in this manner reveals that the isolation between two input ports is 18 dB [9]. In [10], it is shown that two orthogonal modes can be excited by a cross aperture fed by two symmetric feed lines and the isolation between two input ports is better than 27 dB over the operating band. Although this antenna has achieved good performance in both the bandwidth and the isolation, it is complicated in structure because an air bridge is necessary to avoid the intersection between two orthogonal feed lines.

Dual-polarized aperture-coupled antenna with better isolation can be obtained by using multiple coupling apertures, as the multifeed technique is capable of suppressing higher-order modes. One such antenna is reported by Brachat *et al*. in [11], where a dual-polarized aperture-coupled stacked-patch antenna with multiple apertures is presented. One centered aperture fed by the microstrip feed line in used for channel 1, and two apertures fed uniformly in amplitude and phase and positioned symmetrically with respect to the center of the patch, are used for channel 2. This antenna achieves an impedance bandwidth of 20% and the isolation is better than 35 dB over the bandwidth. However all these kind of dual-polarized antennas with multiple apertures are generally more difficult to design and fabricate than the classical dual-polarized antenna with two apertures in [9].

In this chapter, a broad-band dual polarized aperture coupled microstrip antenna is presented. The antenna configuration would first be described and then some of the results, such as the radiation pattern are presented and described.

7.4.2 Design Specifications 1: Antenna Layers

It is a two-port antenna with symmetric structures at two ports. The antenna consists of three dielectric substrate layers 1, 2, and 3 and one air layer as shown in Figure 16.

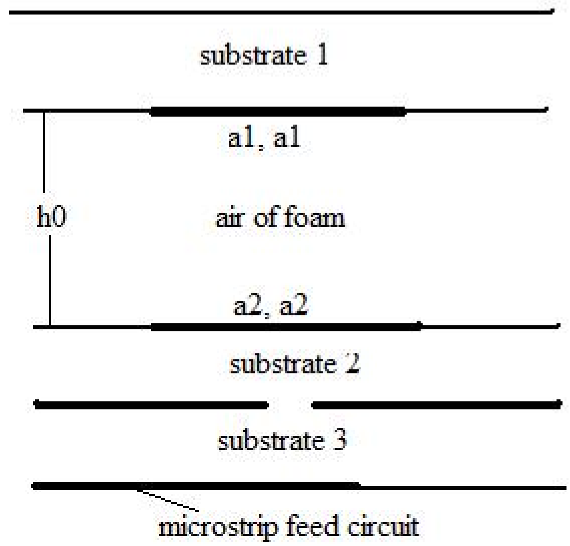

Figure 16. Substrate Layers of the Dual-Polarized Antenna [8].

The upper square patch having a length of a_1 is put on the back of substrate 1. Since the upper square patch in inverted, substrate 1 also acts as the radome for environmental protection. The radome, i.e., substrate 1, has a permittivity of ε_{r1} and a thickness of h_1. The lower square patch having a length of a_2 is mounted on substrate 2 having a permittivity of ε_{r2} and a thickness of h_2.

7.4.3 Design Specifications 2: Ground Plane, Air Layer, Microstrip Lines

An air layer having a thickness of h_0 separates two radiating patches. This air layer can be realized by using a foam substrate or air spacers. The microchip feed lines are put on the back of substrate 3 having a permittivity of ε_{r3} and a thickness of

h_3, while one ground plane is inserted between substrates 2 and 3. The lower radiating patch is excited on the diagonals by two H-shaped apertures.

7.4.4 Design Specifications 3: H-Shaped Aperture Coupling

The lower radiating patch is excited on the diagonals by two H-shaped apertures. The H-shaped aperture is defined by parameters $l_{1,} w_{1,}, l_{2,}$, and w_2, and the offset of aperture from the patch center is *d*, as indicates in Figure 17.

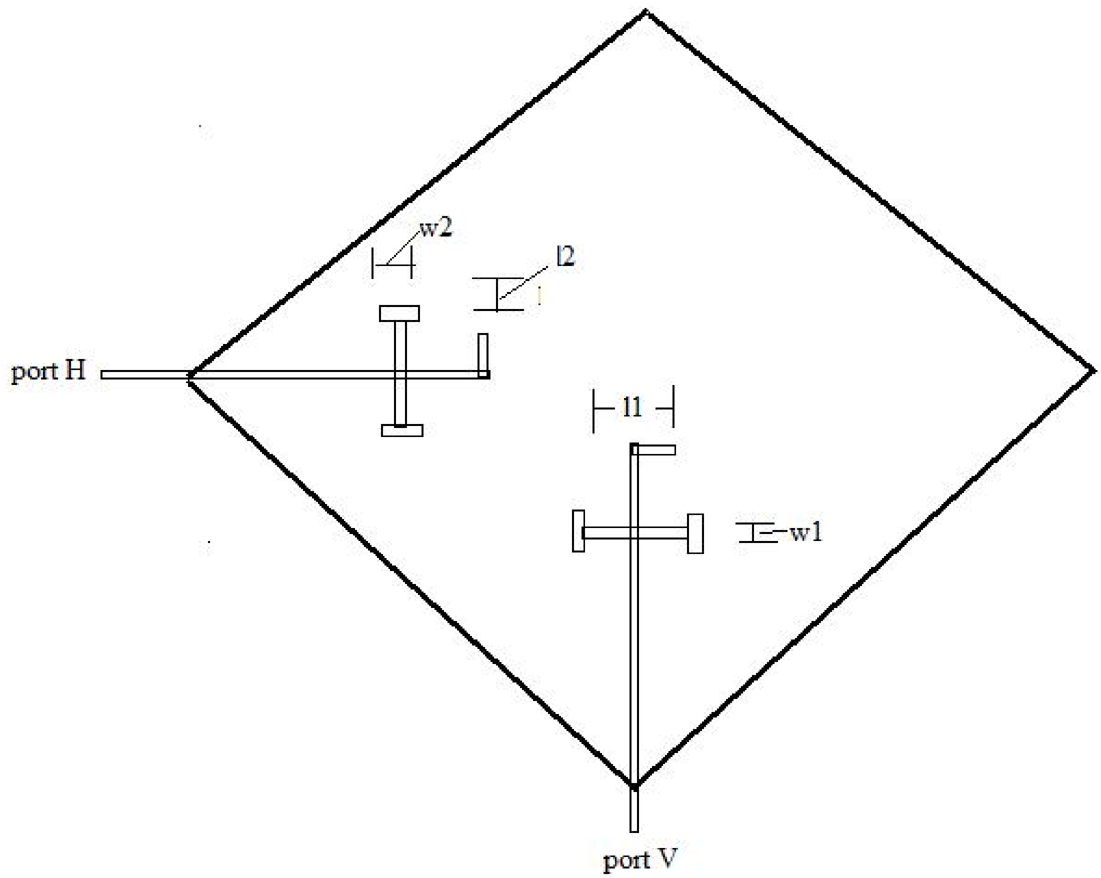

Figure 17. Configuration of the Dual-Polarized Antenna [8].

As the H-shaped aperture has more design freedom than the rectangular aperture commonly used, it is more flexible for antenna performance optimization. Two methods are used together to reduce the backward radiating levels: one is that the resonance of the aperture is chosen to be as far as possible away from the operating band of the antenna. So the wide-band characteristics are produced by the double resonance of stacked patches. The second method is the use of H-shaped aperture, which can lead to improved coupling levels and thus low back-ward radiating level [12].

7.5 Antenna Parameters

The antenna parameters are a_1 = 37 mm, a_2 = 32 mm, ε_{r1} = 2.33, h_1 = 1.6 mm, ε_{r2} = 2.33, h_2 = 1.66 mm, ε_{r3} = 2.2, h_3 = 0.8 mm, h_0 = 7 mm, l_1 = 10 mm, w_1 = 1 mm, l_2 = 3 mm, w_2 = 4 mm, and d = 14 mm. In the bottom layer, the microstrip feed line has a width of 2.4 mm and the microstrip stub extends a total length of 17 mm (not including the microstrip bend) beyond the center of the aperture.

7.6 Results

7.6.1 S21 Parameters

The theoretical results of return loss at port V and H are shown in Figure 18. The highest isolation of 47 dB was obtained at 2.7 GHz.

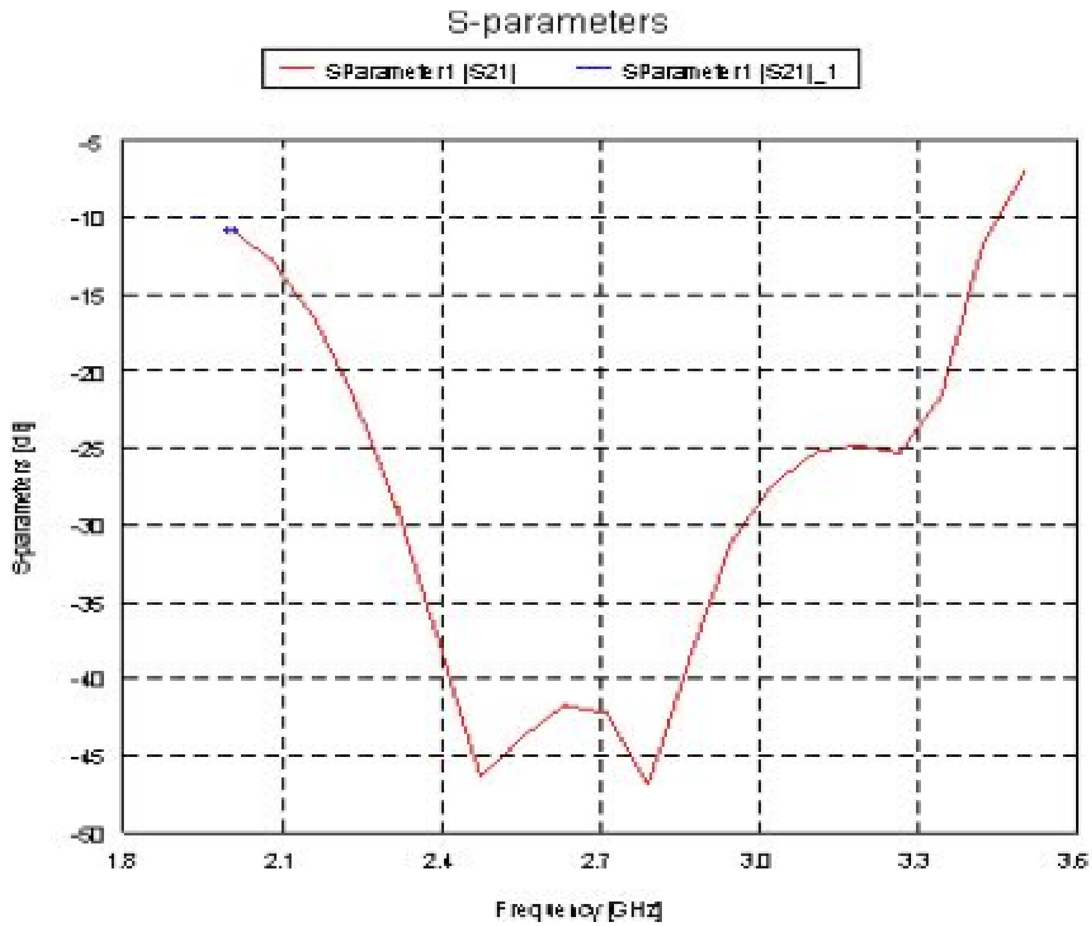

Figure 18. S21 Parameters showing Coupling between Polarization Ports.

7.6.2 Radiation Pattern

The radiating pattern of the electric field is shown in Figure 19. The cross polarization levels are -26.9 dB and -33.6 dB for the *E* and *H* planes respectively. The pattern shows a very directed electric field with almost no back radiation and no side lobes.

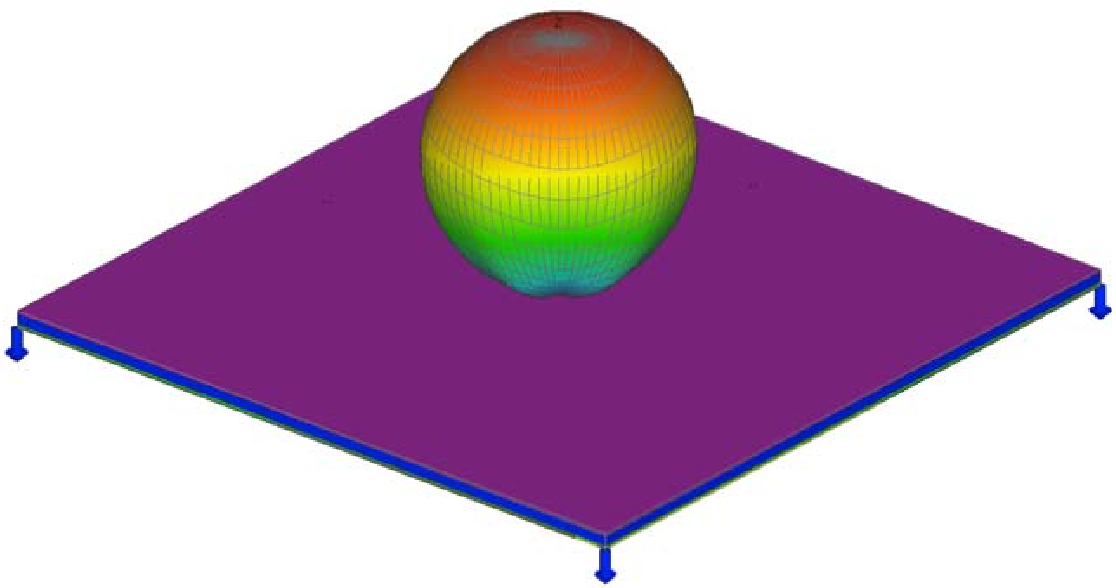

Figure 19. Electric-Field Pattern for the Dual-Polarized Microstrip Patch Antenna.

Chapter 8

SMART ANTENNAS

8.1 Introduction

The term "smart antenna" generally refers to any antenna array, terminated in a sophisticated processor, which can adjust or adapt its own beam pattern in order to emphasize signals of interest and to minimize interfering signals [13]. This concept is opposed to the fixed beam "dumb antenna," which does not attempt to adapt its radiation pattern to an ever-changing electromagnetic environment. Smart antennas have numerous benefits in wireless applications as well as in sensors such as radar. In the realm of mobile wireless applications, smart antennas can provide higher system capacities by directing narrow beam toward the users of interest, while nulling other users not of interest.

In this chapter a novel and alternative approach is discussed where an array of smart antenna is placed on each of the missiles. Using beacons on the ground the missile would be able to calculate the respective theta and phi angles for each of the. This information would enable us to calculate all six degree of freedom of the missile and arrive at a complete solution.

Smart antennas in this scheme can be used to enhance direction-finding (DF) techniques by more accurately finding angles-of-arrival (AOA) [13]. The accurate estimation of AOA is very beneficial in this project for accurately tracking a moving projectile.

8.2 Angle-of-Arrival Projectile Location

This section describes a new method for the location of projectiles in two dimensions. This method assumes that three beacons are situated on the ground in known locations, and that they continually producing signals identifying themselves. The projectiles themselves are assumed outfitted with antenna arrays for angle-of-arrival estimation. The problem is highly complicated in three dimensions so the first step is to solve it in 2-D (the plane). That is the reason at least three beacons are necessary to determine a unique solution in 2-D. This differs from triangulation, which would only require two beacons.

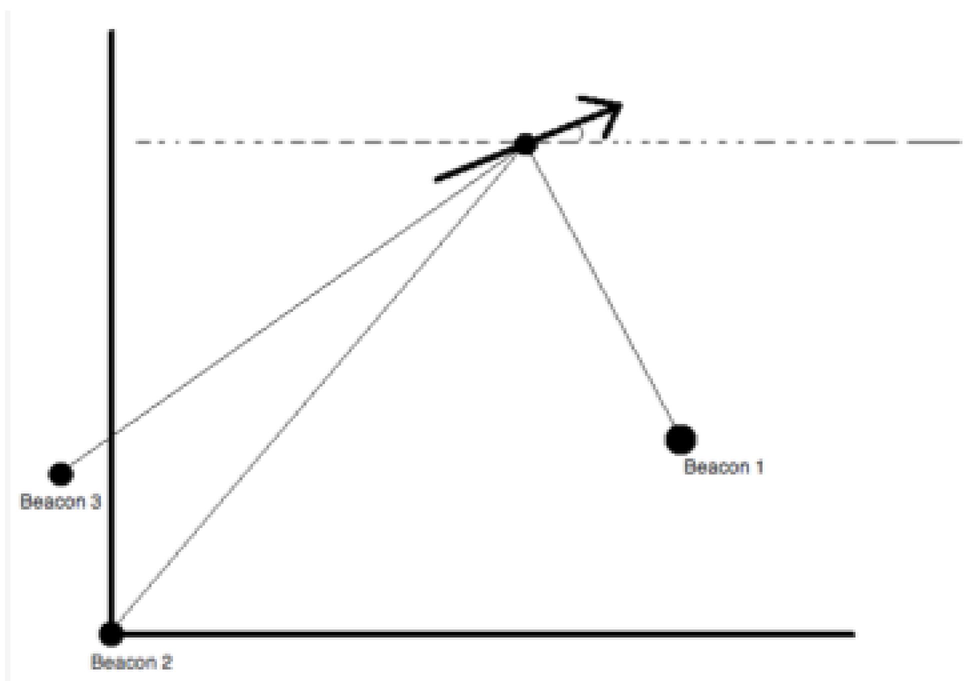

Figure 20. Predicting the Angle and Position of a Missile in 2-D.

The remainder of this section is composed of two parts. The first of these briefly described AOA estimation, and the second shows how angular information can be used to determine the locations and orientation of the projectile.

8.2.1 AOA Estimation

An antenna array is a group of $N > 1$ antenna, working in concert, with signals that can be measured independently [13]. A monochromatic, unit strength plane wave incident on such an array (from an angle θ) generates a signal on each antenna that be measured or computed. Assuming each one of the antenna is used as reference for the definition of phase, the result of this measurement is $\mathbf{a}(\theta)$, a complex vector of N entries giving the signal received on each of the antenna.

Of course, in a practical situation, the signal received will not be monochromatic, nor will it be free of noise. Assuming that the signal source of interest is narrowband, we can write the signal received by the array as:

$$\mathbf{x}(t) = s(t)\mathbf{a}(\theta) + \mathbf{n}(t) \tag{8.1}$$

Where $s(t)$ is the signal generated by the source, and $\mathbf{n}(t)$ is the noise. If instead of a single signal source there ate M sources incident at angles $\theta_1, \theta_2, ..., \theta_m$ carrying signals $s_1(t)$, $s_2(t)$, …, $s_M(t)$, this can be written as:

$$\mathbf{x}(t) = \mathbf{A}(\theta_1, \theta_2, \ldots, \theta_M)\mathbf{s}(t) + \mathbf{n}(t) \tag{8.2}$$

Where, the column vector $\mathbf{s}$ is given by

$$\mathbf{s}(t) = \left[s_1(t) \quad s_2(t) \quad \cdots \quad s_M(t) \right]^T \tag{8.3}$$

(the subscript T denotes transpose), and the $N \times M$ matrix $\mathbf{A}$ is given by:

$$\mathbf{A}(\theta_1, \theta_2, \ldots, \theta_M) = \left[\mathbf{a}(\theta_1) \quad \mathbf{a}(\theta_2) \quad \cdots \quad \mathbf{a}(\theta_M) \right] \tag{8.4}$$

The next step in AOA estimation is the approximation of the covariance matrix; that is, an estimate of the covariance of the signals received by the antennas. The exact covariance matrix is give by:

$$\mathbf{R}^* = \int_{-\infty}^{\infty} \mathbf{x}(t)\mathbf{x}^H(t)dt \tag{8.5}$$

Where the subscript H denotes the conjugate transpose. This cannot be computed (since the future is not known) but there are many ways of approximating it, ranging from taking the current value of $\mathbf{x}(t)\mathbf{x}^H(t)$ as an approximation, or averaging $\mathbf{x}(t)\mathbf{x}^H(t)$ over a finite portion of the past, etc [13]. In any case, several time-varying approximation to $\mathbf{R}^*$ are possible. These will be denoted by $\mathbf{R}(t)$.

Given the covariance matrix, it is possible to compute a pseudospectrum $P(\theta)$ of the desired signals. The units of the pseudospectrum are energy density, and maximizing it gives information on the location of the signal sources. Many different methods can be used for computing $P(\theta)$ [13], but here we describe only one: multiple signal classification, or MUSIC [14]. The MUSIC pseudospectrum is found by first computing the eigenvalues and eigenvectors of $\mathbf{R}(t)$. The largest M eigenvalues are assumed to belong to desired signals, as the remaining N-M eigenvalues are assumed to belong to noise. These vectors may be collected into an $N\times N$-M matrix given as follows:

$$\mathbf{E} = \begin{bmatrix} \mathbf{e}_1 & \mathbf{e}_2 & \cdots & \mathbf{e}_{N-M} \end{bmatrix} \tag{8.6}$$

With columns that span the noise subspace. Since the signals are statistically orthogonal to the noise (this is what makes the noise “noise” rather than signal), the expression in equation 8.7,

$$P(\theta) = \frac{1}{\left|\mathbf{a}^H(\theta)\mathbf{E}\mathbf{E}^H\mathbf{a}(\theta)\right|} \tag{8.7}$$

will be maximized in the direction of desired signals.

In addition, the idea can be extended to identify different signals. In the context of the current problem, this means that different beacons can be identified and located with respect to the projectile.

8.2.2 Projectile Location

To see how AOA estimation can be used to solve the projectile location problem is two dimensions, consider Figure 21. Three beacons are located at the origin and the points (x_1, y_1) and (x_2, y_2). In addition, using AOA estimation, the angle of arrival of the signals from each beacon can be used to find the angles marked ψ_1, ψ_2, and ψ_3. In short all, of the parameters marked in red in the Figure 21 are assumed to be known.

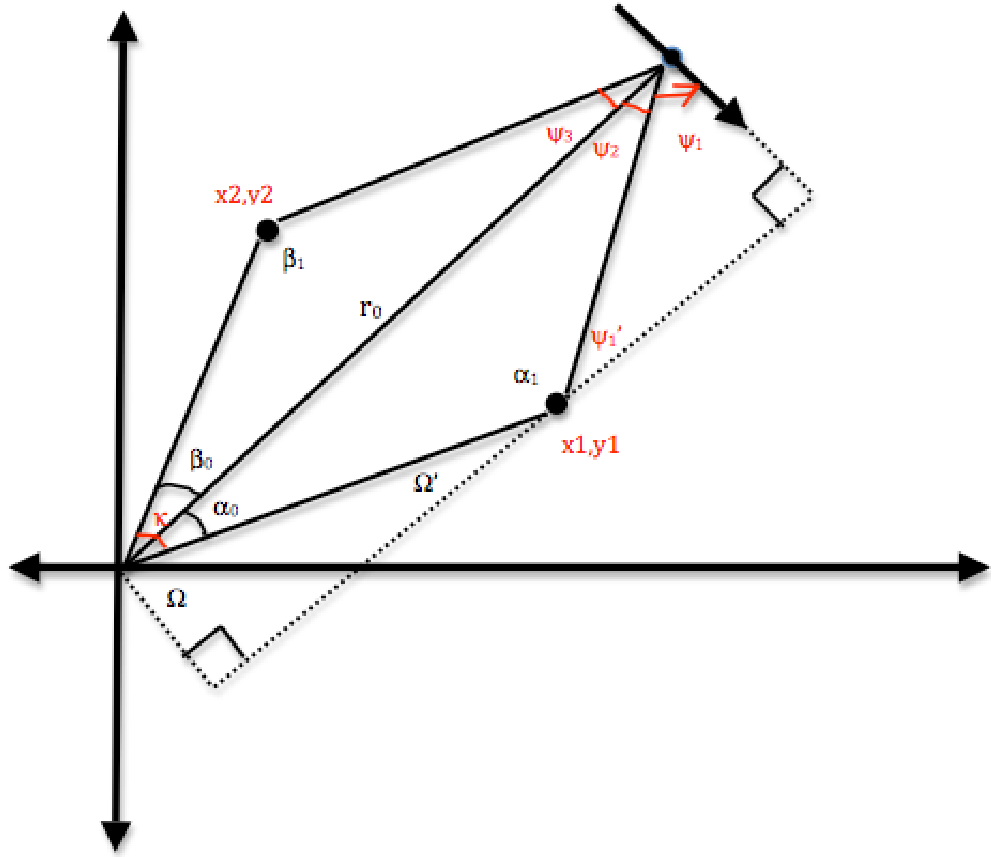

Figure 21. Geometry of Projectile Location.

The most important step in solving the problem s locating the angle labeled Ω in the Figure 21. This is the angle between two vectors: one pointing along the projectile itself, and one from the origin to the point (x_1, y_1). Defining the two angles $\alpha = \psi$ and

$$\beta = 360^{\circ} - \psi_1 - \psi_2 - \psi_3 - \kappa \qquad (8.8)$$

and the two quantities:

$$A = \frac{\sqrt{x_1^2 + y_1^2}}{\sin\psi_2},\ B = \frac{\sqrt{x_2^2 + y_2^2}}{\sin\psi_3} \tag{8.9}$$

The tangent of the desired angle is:

$$\tan\Omega = \frac{B\sin\beta - A\sin\alpha}{A\cos\alpha + B\cos\beta} \tag{8.10}$$

Denoting the angle that the projectile makes with the positive x-axis as ϕ, it is clear from the figure that,

$$\phi = \tan^{-1}\left(\frac{y_1}{x_1}\right) - \Omega \tag{8.11}$$

(Note that unlike all other angles in the Figure 21, ϕ is an algebraic angle, considered negative if the heading is "down" as show in the figure.) The angle ϕ is one of the three pieces of data sought.

Similarly, the angles labeled α_0 and α_1 in the figure are given by:

$$\begin{aligned} \alpha_0 &= 180^{\circ} - \psi_1 - \psi_2 - \Omega \\ \alpha_1 &= \psi_1 + \Omega \end{aligned} \tag{8.12}$$

By the law of sines,

$$r_0 = \frac{\sin\alpha_0}{\sin\psi_2}\sqrt{x_1^2 + y_1^2} \tag{8.13}$$

In terms of these parameters, the coordinates of the missile are given by:

$$x = r_0\cos\left[\alpha_0 + \tan^{-1}\left(\frac{y_1}{x_1}\right)\right] \tag{8.14}$$

$$y = r_0\sin\left[\alpha_0 + \tan^{-1}\left(\frac{y_1}{x_1}\right)\right] \tag{8.15}$$

Chapter 9

SUMMARY AND FUTURE WORK

In this thesis the design of a novel sensor based on the polarization of the electromagnetic wave was presented in order to determine the angular orientation of the body. A through mathematical analysis were discussed and presented that lead to the determination of the three angles of the missile launched in free space. A detailed work was presented that discussed how electromagnetic theory could be brought to an effective use, specially the use of polarization. This did not come without the design of antennas to detect and sense the polarization of the radiated wave. The antenna design was many folds. We started with a simple dipole structure and then built on some more complicated antenna design such as the design of a wide-band aperture couple microstrip patch antenna was presented along with the simulation results. Also towards the end the approach using smart antennas was discussed.

The smart antenna work has a lot of room for further investigation in three dimensions in order to determine not just the angular orientation of the body but also its position and velocity estimation. Some novel antennas could be designed to exploit the antenna radiation patterns to overcome sensitivity and also the off-beam problem.

REFERENCES

[1] J.C. Maxwell, *A Treatise on Electricity and Magnetism*. Oxford: Oxford University Press, 1873.

[2] FEKO, Suite 5.4. [CD-ROM]. Stellenbosh, South Africa.: EM Software & Systems, 2008.

[3] C.A Balanis, *Advanced Engineering Electromagnetics*. New York, NY: John Wiley & Sons, 1989.

[4] C.A Balanis, *Antenna Theory: Analysis and Design*. Hoboken, NJ: John Wiley & Sons, 2005.

[5] H. Goldstein, *Classical Mechanics*. Reading, MA: Addison-Wesley, 2007.

[6] M.E. Mortenson, *Geometric Modeling*. New York: John Wiley & Sons, 1997.

[7] P.S. Nakar. "Design of a Compact Microstrip Patch Antenna for use in Wireless/Cellular Devices." Masters Thesis, Florida State University, 2004.

[8] S. Gao, L.W. Li, M.S. Leong, and T.S. Yeo, "A broad-band dual polarized microstrip patch antenna with aperture coupling," *IEEE Transactions on Antennas and Propagation*, vol. 51, pp. 898-900, 2003.

[9] A. Adrian and D.H. Schaubert, "Dual aperture-coupled microstrip antenna for dual or circular polarization," *Electron. Lett*., vol. 23, pp. 1226-1228, 1987.

[10] C.H. Tsao, Y.M. Hwang, F. Kilburg, and F. Dietrich, "Aperture-coupled patch antenna with wide-bandwidth and dual-polarization capabilities," *IEEE Transactions on Antennas and Propagation,. Symp. Dig.*, 1988, pp. 936-939.

[11] P. Brachat and J. Baracoo, "Printed radiating element with two highly decoupled input ports," *Electron. Lett.*, vol. 31, pp. 245-246, 1995.

[12] D.M. Porzar and S.D. Targonski, "Improved coupling fo aperture-coupled microstrip antennas," *Electron. Lett.*, vol. 27, no. 13, pp. 1129-1131, 1991.

[13] F. Gross, *Smart Antenna for Wireless Communications*. New York: McGraw-Hill, 2005.

[14] L. Godara, “Applications of antenna arrays to mobile communications: beamforming and direction of arrival consideration,” *Proceedings of the IEEE*, vol. 85, no. 8, pp. 1195-1245, 1997.

[15] R. Schmidt, “Multiple emitter location and signal parameter estimation,” *IEEE Transactions on Antennas and Propagation*, vol. AP-34, no. 2, pp. 276-280, 1986.